Geoscience Letters

RESEARCH LETTER

Open Access

Characterization of landslides: a vertical electrical sounding approach

W. A. P. P. Christopher[1*], Nalin De Silva[2], A. M. A. N. B. Attanayake[1] and Pathmakumara Jayasingha[3]

Abstract

The high groundwater activity typically found in landslide bodies favors electrical resistivity methods to characterize the subsurface of landslides. The more water present, the more the current injection into the ground and thus greater the depth of penetration. Furthermore, this generates a higher contrast between the stable and the unstable mass of the landslide. Being a cost-effective and a flexible approach to characterize landslides, 1-D electrical resistivity surveys have the ability to acquire point data similar to borehole logs, thus allows to detect and highlight anomalies of groundwater flow and groundwater build up. These parameters could change from point to point due to the inherit disturbed nature of landslides. A preliminary vertical electrical sounding survey using Schlumberger electrode configuration was carried out along the axis of a creep-type landslide in Badulusirigama, Badulla, Sri Lanka. Four survey points were established for the preliminary VES survey. Each survey line spanned 140 m in length. The data revealed the presence of two types of layers with high (200–370 Ω m) and low (20–60 Ω m) apparent resistivities. Another resistive layer with an apparent resistivity around 100–140 Ω m was found to be sandwiched in the clay layer which was significant to the landslide body and interestingly was not observed in the borehole logs. Furthermore, the southwest inclination of this sandwiched layer explained the southwest region of the landslide being highly active in terms of groundwater discharge through horizontal drains. The bedrock was not detected at three of the survey points highlighting the thick clay layer present in the landslide body. This preliminary survey revealed the general anatomy of the landslide along its axis in terms of the number of layers, type of layers, their thicknesses, the presence of water, and their resistivities.

Keywords Landslides, Vertical electrical sounding, Apparent resistivity

Introduction

A landslide is a mass movement of earth material driven by gravity. They are classified based on the type of material being displaced and type of movement which includes falls, topples, slides, flows, and lateral spreads (Varnes 1978). In most cases one or more types of these movements are found to be involved in landslides which can be described as a complex movement. Forces which cause a landslide to occur are called triggering factors and these vary between natural causes, such as precipitation, earthquakes, and volcanic activities to human activities, such as improper land use (Gill and Malamud 2014). These triggering factors tend to result an imbalance between the forces driving the failure and forces that are resisting the movement and will favor failure when the driving forces overwhelm the resisting forces involved.

The concept of the factor of safety is developed based on the ratio between the sum of resisting forces and the sum of diving forces acting on a particular earth material mass on a slope due to gravity. Precipitation, the major triggering factor of landslides, causes the driving forces

*Correspondence:
W. A. P. P. Christopher
wapchristopher@gmail.com
[1] Department of Applied Earth Sciences, Uva Wellassa University, Badulla, Sri Lanka
[2] Geological Survey and Mines Bureau, Pitakotte, Sri Lanka
[3] Department of Geography, University of Colombo, Colombo, Sri Lanka

to increase while decreasing the resisting forces. With increasing water content in soil, the friction angle of that particular soil decreases and causes the soil to achieve stability at an angle less than that of the soil when it is dry. Adding to the adversity, a series of transformations causes the soil to surpass the liquid limit after which the particular soil behaves similar to a liquid. First, a thin film of water develops on the surface of the soil particles as water is introduced to a certain mass of dry soil (Fig. 1). This phenomenon is called as adsorption.

As the water content increases further the voids among soil particles are filled with water and the soil achieves saturation. When more water is introduced, water generates pressure in the pores (pore water pressure) which acts outwards on the soil particles. This pushes the soil particles away from each other and causes the friction to decrease by the reduction and finally the loss of grain-to-grain contacts. The pore water pressure (u) further reduces the normal stress (σ) and the resulting stress is called as "Effective normal stress (σ')" (Lu et al. 2010) which is always less than the dry normal stress and is given by

$$\sigma' = \sigma - \mathrm{u}$$

or in terms of forces

$$\sigma' A = \sigma A - uA = W \cos\beta - uA.$$

The accumulation of water in voids in between soil particles adds to the weight of the soil making wet soil heavier than an equivalent volume of dry soil. This increases the driving forces. This phenomenon where the driving forces increase while resisting forces decrease is initiated with the introduction of water to a dry slope. The natural source which dumps water onto the earth's surface is precipitation and it triggers the adverse chain of transformations in soil described above which ultimately could lead to a landslide. Thus, detection of presence and activity of water is crucial in mitigating landslides.

Currently, borehole logs are used to delineate the subsurface of landslides. Due to this approach being costly and time consuming, only a few boreholes are drilled. The conventional interpolation technique is then followed to generate the sub surface profile in between the boreholes. The inherit disturbed nature of the landslide suggests that critical parameters, such as groundwater flow, groundwater accumulation, and the geology, could change even over a small area of the landslide body. Thus, interpolating between boreholes in such a disturbed body could easily misinterpret the real anatomy of the landslide subsurface.

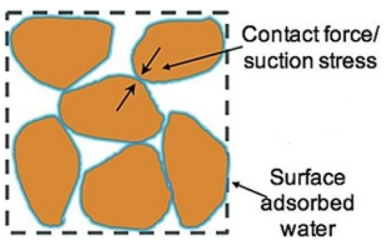

Fig. 1 Adsorption (Lu and Mitchell 2019)

Geophysical approaches seems to be ideal to solve this issue as they would provide data over an area (Everett 2013; Kearey et al. 2001). Furthermore, the abundance of water present in landslide masses favors electrical resistivity methods over other geophysical methods, such as seismic reflection (Bruno and Marillier 2000; Ferrucci et al. 2000; Bichler et al. 2004), seismic refraction (Kearey et al. 2002), seismic tomography (Meric et al. 2005), electromagnetic methods, Ground Penetrating Radar (GPR) (Bichler et al. 2004), and gravimetric studies (Del Gaudio et al. 2000). The more water present, the higher the current injection into the ground and thus the deeper the penetration depth. Thus, before conducting an advance 2-D ERT survey a preliminary 1-D survey would reveal the most basic but vital data such as the number of layers, type of layers, their thicknesses, the presence of water, and their resistivities. Furthermore, a geological profile could be developed based on the apparent resistivity curves which could then be correlated with the geological profile developed based on borehole data. This set of correlated data then could be used as a site specific key to delineate the subsurface at any given point on that particular landslide. This eliminates the need for multiple boreholes to be drilled and in turn would be economical and time saving.

The site

The Badulusirigama landslide is a deep-seated landslide located adjacent to the Uva Wellassa University premises in the Southeastern flank of the Central Highlands of Sri Lanka (Lat/Lon 6.980315 N/81.075787 E) (Fig. 3). The landslide covers an area of around 18 acres and sits at an elevation of 790 m above mean sea level in the Badulusirigama village (Nature based landslide risk management project in Sri Lanka, 2019).

The source rock in the region is a quartzofeldspathic gneiss (057/17). Three layers corresponding to a weathering profile were identified from 6 borehole surveys conducted by the NBRO (Fig. 13): A colluvium with a thickness of around 9–13 m, a highly weathered layer beneath the colluvium with a thickness varying from 5 to 15 m, and a slightly to moderately weathered rock layer at the base (Monitoring Report No. 8 May 2016, NBRO). This particular site was selected with the objective of comparing and contrasting the geological

Table 1 Electrode spacing

AB/2 (m)	1.5	2	3	3	5	7	10	10	15	20	30	40	50	50	70
MN/2 (m)	0.5	0.5	0.5	1	1	1	1	2.5	2.5	2.5	2.5	2.5	2.5	7	7

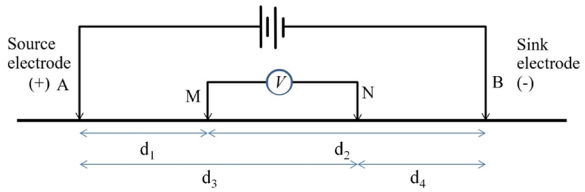

Fig. 2 Schlumberger array setup (A & B: Current electrodes, M & N: Potential electrodes) (Rolia and Sutjiningsih 2018)

profile developed by borehole data with the VES profiles developed.

Methodology

Four 1-D VES surveys (P1, P2, P3, and P4) were carried out along the axis of the landslide from its crest to the toe (Fig. 3). Each survey line spanned for 170 m in length. Current electrode spacing (AB/2) and potential electrode

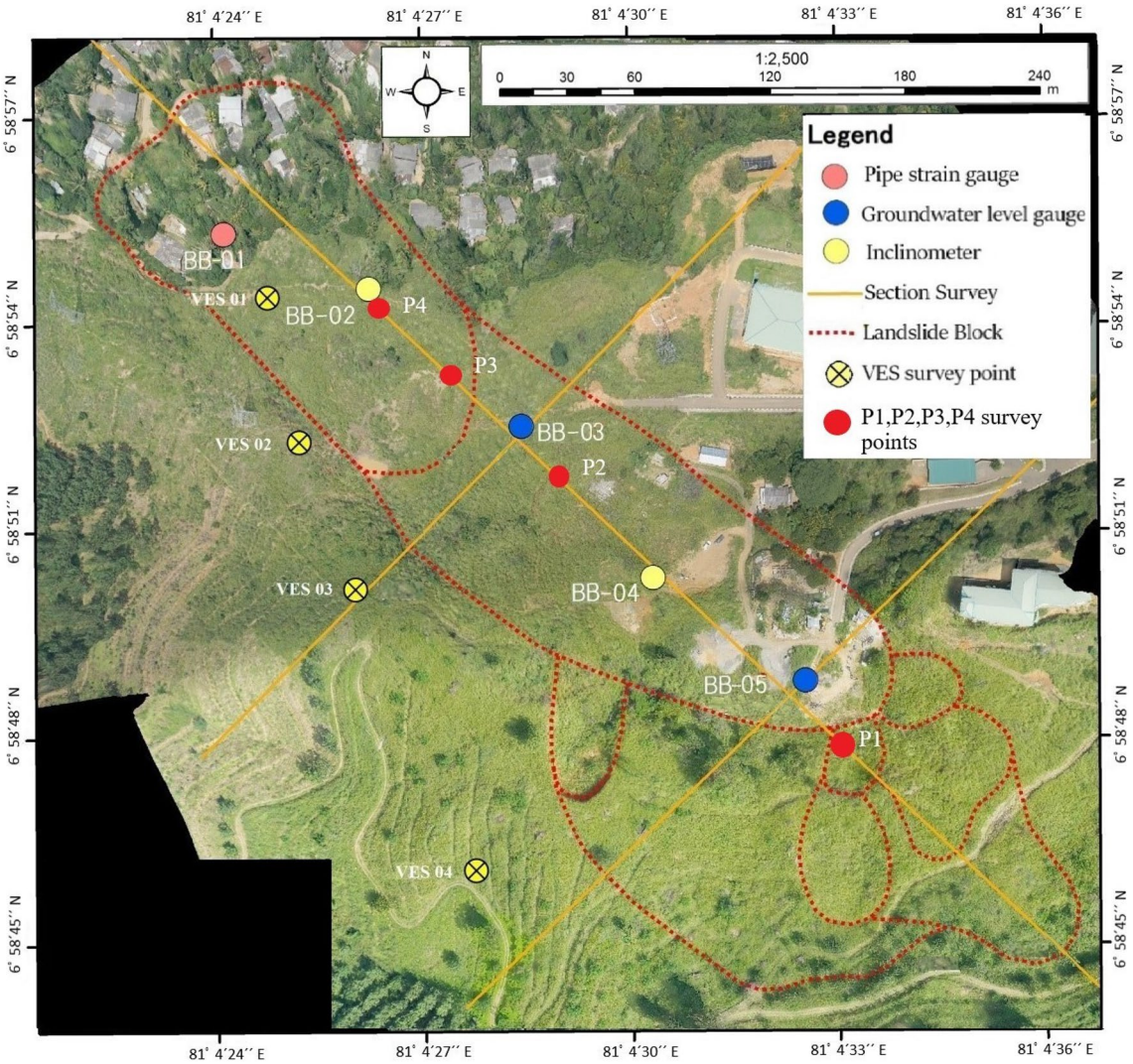

Fig. 3 Landslide area shown on a drone image (Landslide Research and Risk Management Division, NBRO)

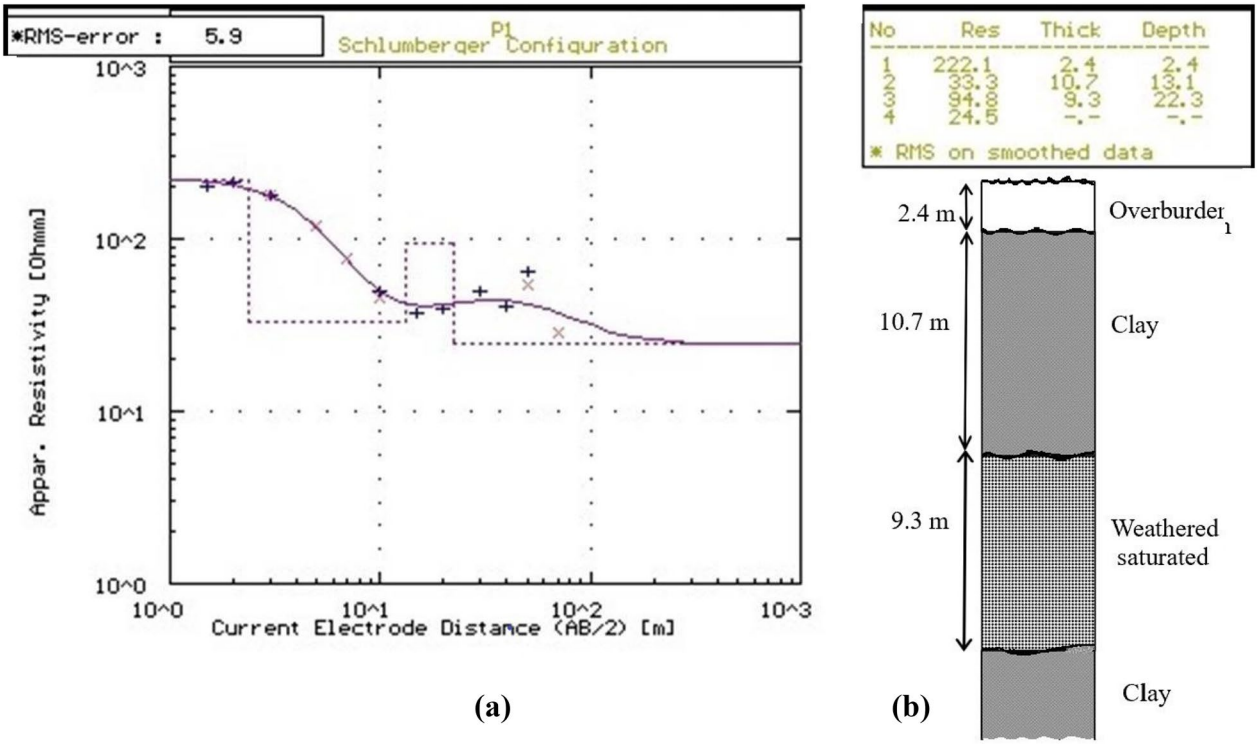

Fig. 4 **a** Curve matched from RESIST software for P1, **b** Geological profile for P1

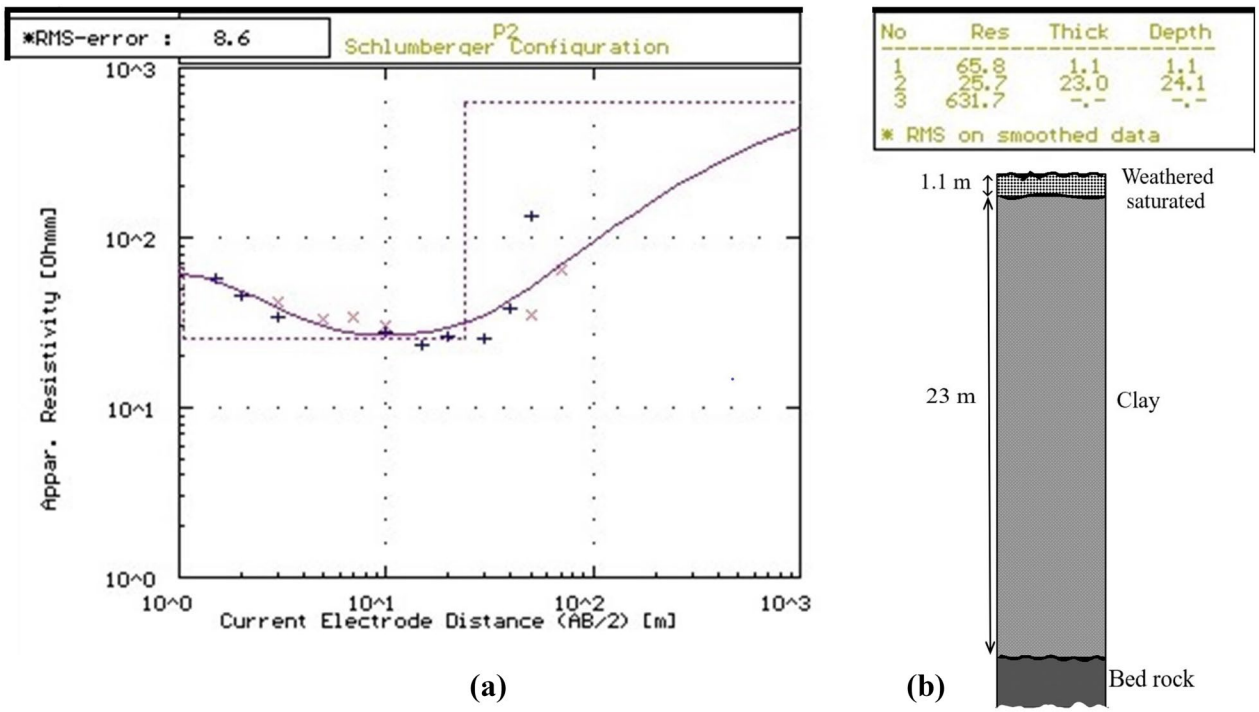

Fig. 5 **a** Curve matched from RESIST software for P2, **b** Geological profile for P2

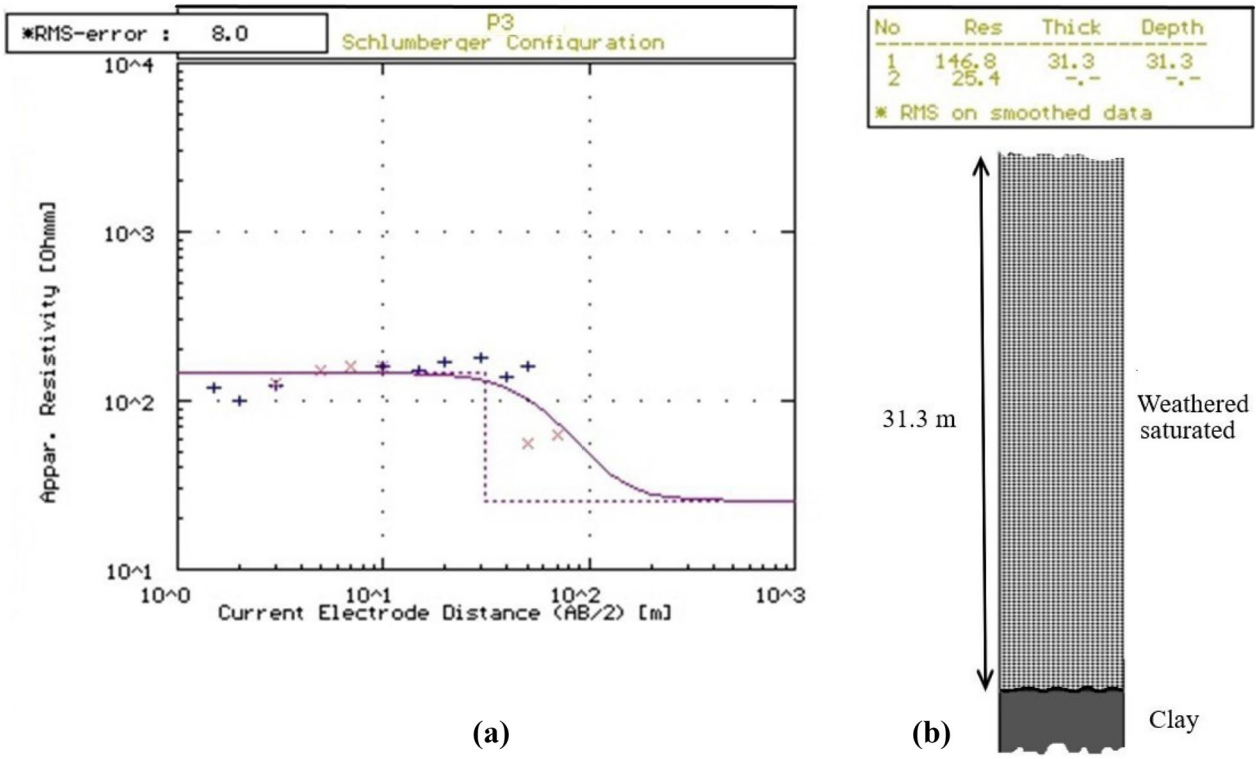

Fig. 6 **a** Curve matched from RESIST software for P3, **b** Geological profile for P3

spacing (MN/2) followed in the survey are given in Table 1.

The potential difference (V) between M and N potential electrodes is given in Eq. (1) (AL-Menshed 2018).

$$V = \frac{I\rho}{2\pi}\left(\frac{1}{d_1} - \frac{1}{d_2} - \frac{1}{d_3} + \frac{1}{d_4}\right), \tag{1}$$

where ρ is the apparent resistivity, I is the current, d_1, d_2, d_3, and d_4 are the distances between electrodes (Fig. 2).

By rearranging,

$$\rho = \frac{2\pi V}{I}\left(\frac{1}{d_1} - \frac{1}{d_2} - \frac{1}{d_3} + \frac{1}{d_4}\right)^{-1}. \tag{2}$$

The geometrical factor (k) is given by

$$k = 2\pi\left(\frac{1}{d_1} - \frac{1}{d_2} - \frac{1}{d_3} + \frac{1}{d_4}\right)^{-1}. \tag{3}$$

And thus, the apparent resistivity is given by

$$\rho = \frac{kV}{I} \tag{4}$$

where $V/I = R$ (resistance) (AL-Menshed 2018).

The geometrical factor k was calculated using Eq. (3) and the distances (d_1, d_2, d_3, and d_4) between potential electrodes (AB) and current electrodes (MN). The apparent resistivity values were calculated from the measured resistance values and the geometrical factor values were calculated from the survey based on Eq. (4) (Table 2). The corresponding apparent resistivity curves were plotted on a logarithmic scale using the RESIST software (Van-der Velpen and Sporry 1993) and Microsoft Excel. The matched curves were used to determine the number of layers, their apparent resistivity values, layer thicknesses, and depth to each layer (Fig. 3).

Results and discussion

Three zones with high apparent resistivity, low apparent resistivity, and apparent resistivity around 90–140 Ω m were found at survey point P1 (Fig. 4). The overburden shows a relatively high apparent resistivity around 225 Ω m compared to the clay layer which sits beneath it. But, the apparent resistivity of the overburden on the landslide is significantly low compared to the apparent resistivity values of the overburden (400–600 Ω m) found on the stationary mass outside the landslide. A highly weathered water bearing layer (clay) with a thickness of around 10 m and with significantly low apparent

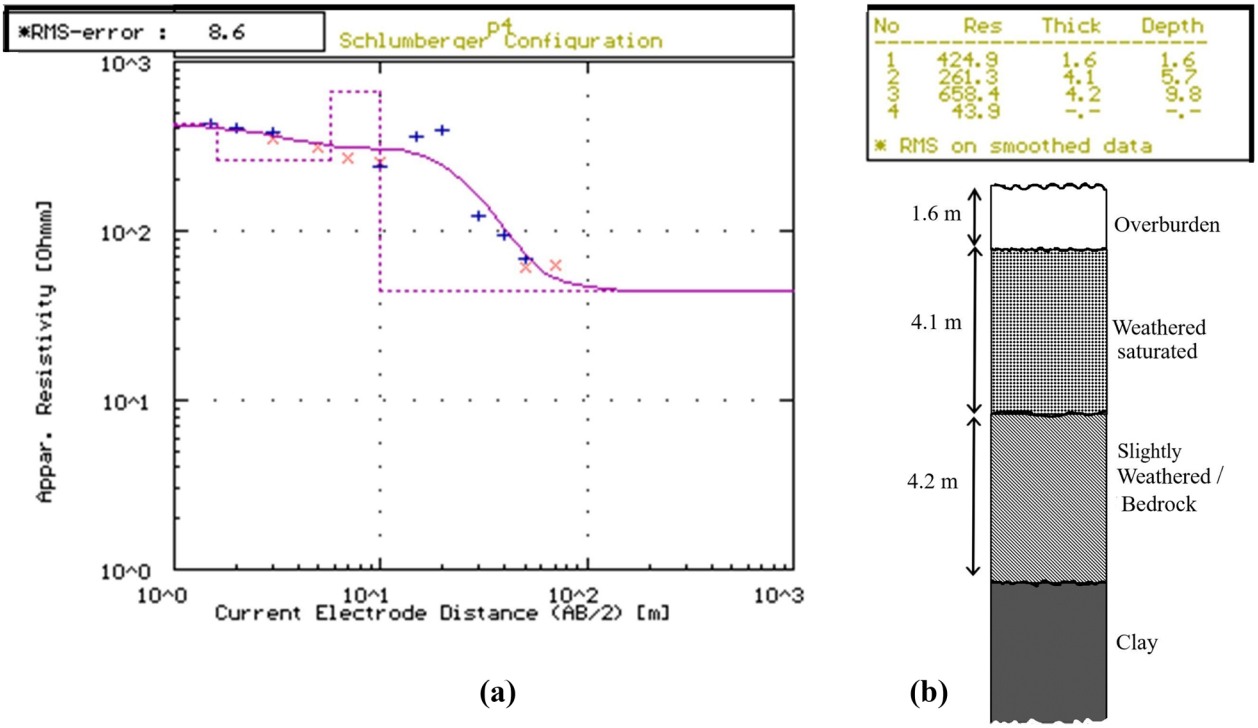

Fig. 7 **a** Curve matched from RESIST software for P4, **b** Geological profile for P4

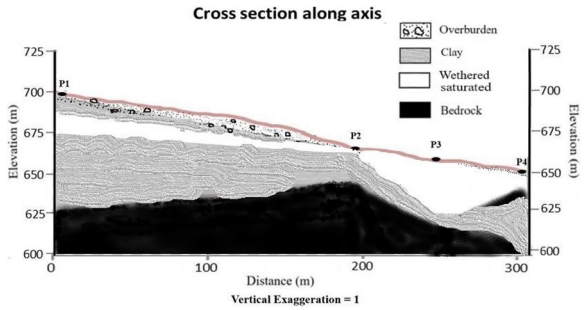

Fig. 8 Interpreted geological profile along survey points P1, P2, P3, and P4

resistivity around 35 Ω m is present below the overburden. Another formation lies below this layer at a depth around 13 m with an apparent resistivity about 95 Ω m, which suggests the presence of fresh water (Saad et al. 2012). This could be a weathered layer saturated with water. And the clay layer can be seen beneath this layer repeating itself. Bed rock is not detected at the surveyed depth at P1.

The weathered saturated layer is almost exposed to the surface at survey point P2 (Fig. 5). The clay layer is around 23 m thick at this survey point. The relatively high apparent resistivity values and the trend of the curve forming the characteristic near 45° ascend at the end marks the bedrock. At P3, the apparent resistivity values around 140 Ω m and the near horizontal trend of the curve (the conductivity through water is constant) (Fig. 6) suggest the presence of fresh water (Saad et al. 2012). The characteristic clay layer continues from P1 and P2 and could be seen at a depth around 31 m at the survey location P3.

At P4, the weathered saturated layer with an apparent resistivity around 260 Ω m is seen below a thin overburden and it transitions to a layer with a higher apparent resistivity which is around 650 Ω m. This could be a representation of a weathering profile where weathering reduces with depth and resistivity rises simultaneously reflecting the intact rock beneath.

Similar to the survey location P1, the alternating high and low resistivity layers are seen at survey point P4 (Fig. 7). The clay layer is present at a depth around 10 m beneath the resistive layer which should be a residual body left from the weathering process. This clay layer is visible at all survey points and sits relatively shallower in the landslide body compared to locations outside the landslide boundary (Christopher et al. 2020). The bed rock is not detected at P1, P3, and P4 locations in the landslide mass. This might either be because the depth of penetration yielded by the electrode configuration used is not sufficient or the bed rock is located further deep in the landslide body compared to the survey locations outside (VES 02, 03, and 04) the landslide where the bed

Table 2 Measured resistance values and calculated resistivity values

AB/2 (m)	MN/2 (m)	*k*	P1 Apparent resistivity (Ω m)	P2 Apparent resistivity (Ω m)	P3 Apparent resistivity (Ω m)	P4 Apparent resistivity (Ω m)
1.5	0.5	6.300	200.5231	56.7497	120.1126	428.6039
2	0.5	11.800	210.6921	45.2569	101.0738	404.9111
3	0.5	27.489	167.1433	34.2995	121.2132	379.1871
3	1.0	12.566	177.8997	42.1899	125.3367	348.5216
5	1.0	37.699	117.7500	33.2648	149.3622	307.5503
7	1.0	75.398	77.22403	33.7432	158.3006	270.7107
10	1.0	155.510	44.8748	30.7080	158.0644	252.1877
10	2.5	58.905	49.97347	27.6534	161.2447	242.0847
15	2.5	137.500	37.54622	22.9842	149.3207	356.7749
20	2.5	247.500	39.3750	25.8026	167.1195	392.9798
30	2.5	562.000	49.49515	25.1692	178.8924	123.4805
40	2.5	1001.000	41.07558	38.6438	137.7926	93.0181
50	2.5	1567.000	65.43489	132.4376	160.0077	68.9900
50	7.0	549.724	53.51975	34.7194	56.1659	60.2767
70	7.0	1088.010	28.70739	63.8129	62.5293	62.5293

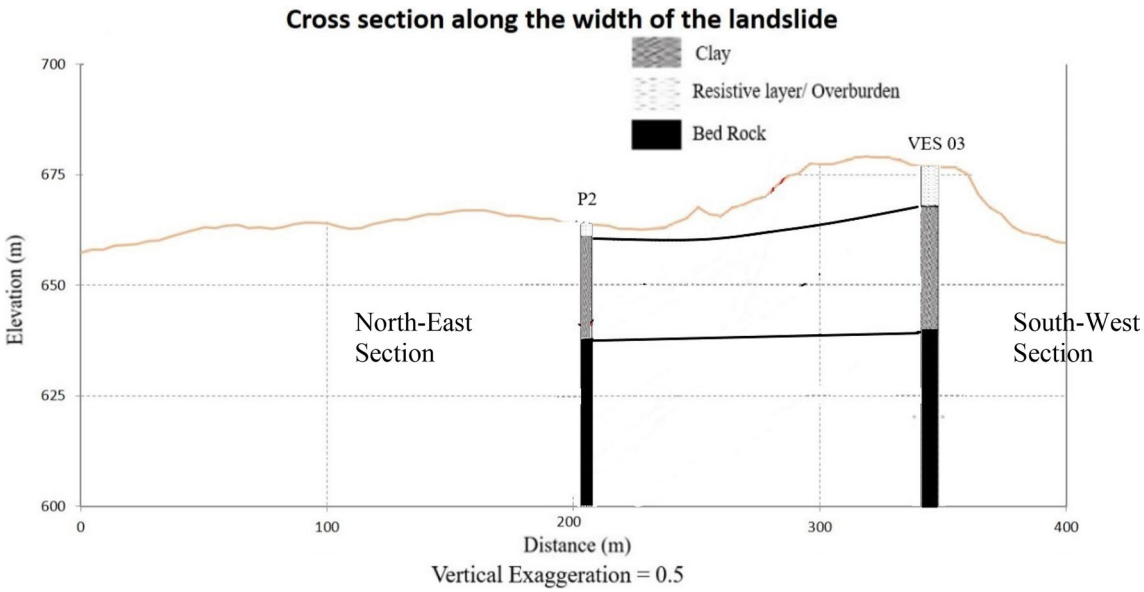

Fig. 9 Cross section of the subsurface across the width of the landslide between P2 and VES 03

rock was found at a depth around 31–40 m (Christopher et al. 2020).

The weathered saturated layer sandwiched in the clay layer is a significant feature seen in the resistivity profiles of P series survey points (Figs. 8, 9, 10). A similar anomaly was detected during the first VES series survey at survey point VES 01 (Fig. 11; Christopher et al. 2020) and the data gathered in the later P series survey supports the fact that it is truly an anomaly rather than an error in data acquisition. This slightly resistive anomaly which has an apparent resistivity more than the apparent resistivity of clay was not observed in the VES series survey points which were located in the stationary mass (VES 02, VES 03, and VES 04). This might explain why the northeast section of the landslide was found dry compared to the southwest section which had highly active horizontal

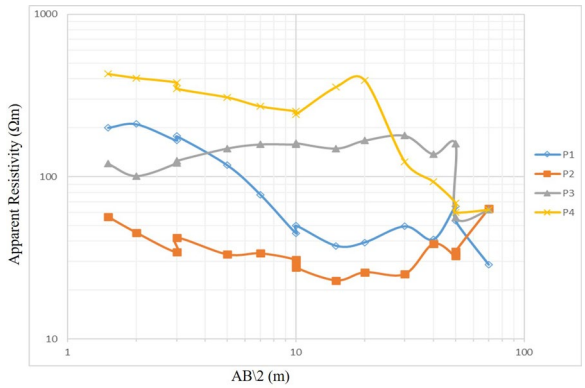

Fig. 10 Apparent resistivity curves of the four VES points (P1, P2, P3, and P4)

drains. The inclined orientation of the bedrock along the southwest direction (Fig. 9) could direct groundwater flow southwest bound, resulting in the southwest section to have highly active horizontal drains.

Another significant observation made is that all the layers present in the landslide mass tend to show relatively low resistivity values compared to locations outside the landslide boundary. This is clearly highlighted in Fig. 12 where resistivity curves corresponding to the survey points on the landslide body (P1, P2, P3, and P4) are below the resistivity curve corresponding to the survey point VES 02 which is located outside the landslide body. Similar observations were made by Caris and Van Asch in a 1-D VES study conducted in 1991. This could be due to the abundance of groundwater present in the landslide body compared to the stationary mass outside the landslide boundary. Additionally, the orientation of the weathered saturated layer (Fig. 8) might be the reason for

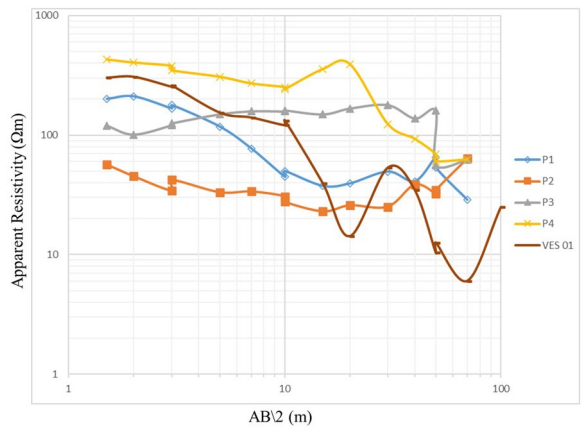

Fig. 11 Apparent resistivity curves of the four VES points (P1, P2, P3, and P4) versus the apparent resistivity curve of survey location VES 01. (Note that VES 01 curve has the same disturbed nature as the survey points P1, P2, P3, and P4)

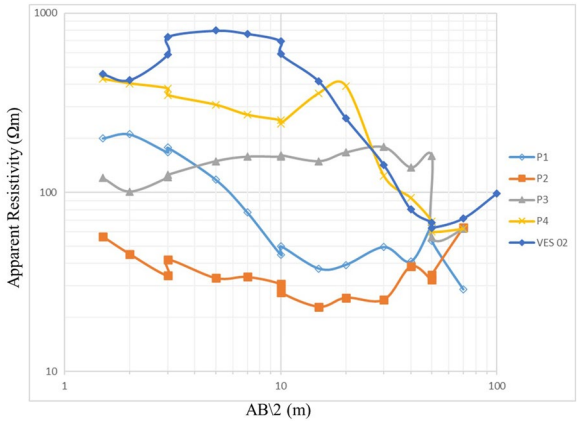

Fig. 12 Apparent resistivity curves of the four VES points (P1, P2, P3, and P4) versus the apparent resistivity curve of survey location VES 02. (Note that VES 02 curve is much smoother and follows a certain trend oppose to curves at survey points P1, P2, P3, and P4 with a highly disturbed trend)

the horizontal drain near P2 location to yield the highest flow rate over a long period of time.

Correlation between the geological profiles developed based on borehole data and VES data

Figure 13 illustrates a geological cross section derived by interpolating data from six borehole surveys conducted along the axis of the landslide by the National Building Research Organization. The four 1-D VES survey points (P1, P2, P3, and P4) along the same axis are marked on the cross section for a comparison of the borehole-derived profile and the VES profiles. At survey point P1, the overburden with a thickness of around 2.4 m and the clay layer with a thickness of around 10.7 m seems to accurately represent the thicknesses of the respective layers in the borehole data-derived section (Fig. 4). But at P2 the thicknesses clearly do not complement each other. The overburden thickness at P2 is much greater than the suggested 1 m by the VES profile and the clay layer is much thicker at around 23 m in the VES profile (Fig. 5) as opposed to the geological cross section. In this example one of either of the interpretations can be wrong since the geology of the location in question is developed by interpolation between two boreholes. And in a highly disturbed body the geological profile could change within a short distance in any direction.

Survey point P3 has the same behavior as the survey location P2. Finally at the survey point P4, the thickness of the colluvium in the geological cross section closely matches the thicknesses of the total thickness of the overburden and the weathered saturated layer (~ 5.7 m) combined together in the VES section (Fig. 7). This is because the resistivity corresponds to geophysical layers rather

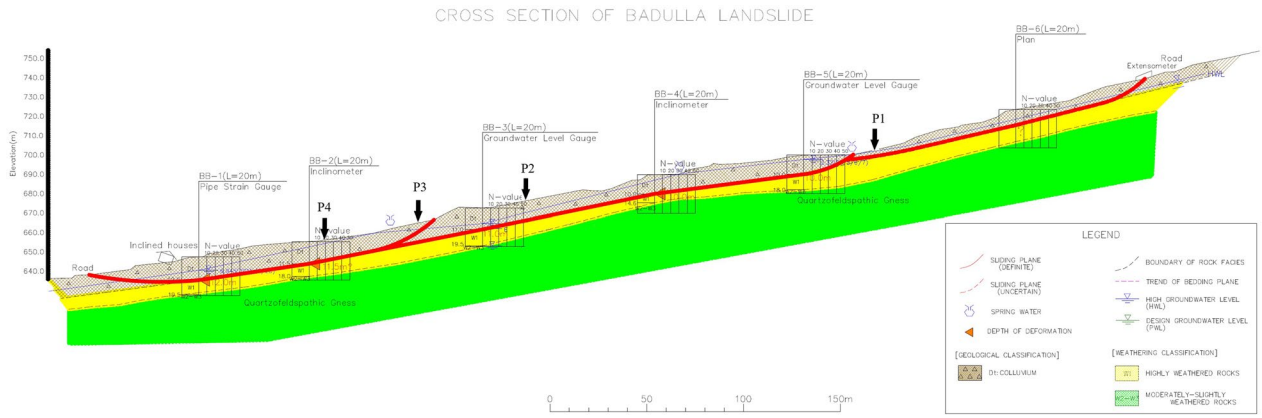

Fig. 13 Borehole-derived geological cross section of the landslide (Landslide Research & Risk Management Division, NBRO)

than geological layers. The colluvium is detected as two separate layers by the resistivity meter due to the partial saturation of the layer.

Conclusion

This study revealed the basic subsurface structure of the landslide along its axis. It is clear that 1-D VES surveys are effective and efficient in generating a first approximation about the number of layers, their thicknesses, the presence of the water-bearing layer and the depth to the bed rock. Apparent resistivity values in the landslide body were lower compared to the stationary mass outside the landslide boundary. This is highlighted in Fig. 12 by the flatter trend of the apparent resistivity curves relevant to the survey points located in the landslide body (P1, P2, P3, and P4) compared to the ones out on the stationary mass (VES 02). This is due to the abundance of water present in the landslide mass which lets the current flow through water in pore spaces rather than through soil particles, which causes the current to flow against a constant resistivity value which does not increase with the depth. The clay layer is present along the axis of the landslide (owing to the presence of feldspathic gneiss in the region which has a high weathering capacity). The southwest sloping weathered saturated layer sandwiched in the clay layer could be the reason for the landslide to be dry on the northeast section and wet on the southwest section.

VES surveys are a quick, cost-effective and a flexible method of delineating the subsurface of a landslide at a given point compared to borehole investigations. However, a more precise picture of the landslide body can be derived by using both borehole investigations and VES surveys combined. Together, borehole logs would reveal the accurate thicknesses of layers involved at specific points, while the VES data would reveal the presence of groundwater at those points. Thus, the ability of VES surveys to be used in filling the gaps between borehole surveys could be studied in future research. The potential misinterpretations occurring from interpolating between boreholes could be minimized as a result.

Supplementary Information

The online version contains supplementary material available at https://doi.org/10.1186/s40562-023-00274-x.

Additional file 1. Resistivity Calculation.

Acknowledgements

The authors would like to thank the Landslide Research & Risk Management Division of National Building Research Organization of Sri Lanka for allowing access to primary data and the Mineral Surveys division of the Geological Survey and Mines Bureu of Sri Lanka for data analysis.

Author contributions

W.A.P.P. Christopher and Nalin De Silva performed the field survey. All the authors contributed with their expertise to interpret data gathered in the survey and to the preparation of the manuscript. All the authors have read and approved the final manuscript.

Funding

This study is a self-funded research.

Availability of data and materials

All data generated or analyzed during this study are included in this published article [and its Additional file 1].

Declarations

Competing interests

The authors declare that they have no competing interests.

Received: 3 November 2021 Accepted: 2 April 2023
Published online: 15 April 2023

References

Agnesi V, Camardab M, Conoscentia C, Di Maggio A, Dilibertoc I, Madoniac P, Rotiglianoa E (2005) A multidisciplinary approach to the evaluation of the mechanism that triggered the Cerda landslide (Sicily, Italy). Geomor 65:101–116

AL-Menshed F (2018) How to understand theoretical background of electrical resistivity method in a simple way

Bichler A, Bobrowsky P, Best M, Douma M, Hunter J, Calvert T, Burns R (2004) Three-dimensional mapping of a landslide using a multi-geophysical approach: the Quesnel Forks landslide. Landslides 1(1):29–40

Bogoslovsky VA, Ogilvy AA (1977) Geophysical methods for the investigation of landslides. Geophysics 42:562–571

Bruno F, Marillier F (2000) Test of high-resolution seismic reflection and other geophysical techniques on the Boup landslide in the Swiss Alps. Surv Geophys 21:333–348

Caris JPT, Van Asch Th WJ (1991) Geophysical, geotechnical and hydrologicalinvestigations of a small landslide in the French Alps. Eng Geol 31:249–276

Christopher WAPP, Harankahawa SB, De Silva N, Attanayake AMANB, Jayasinghe P (2020) Characterization of landslides: a preliminary vertical electrical sounding approach. JGSS 21(2):81–89

Del Gaudio V, Wasowski J, Pierri P, Mascia U, Calcagnile G (2000) Gravimetric study of a retrogressive landslide in southern Italy. Surv Geophys 21:391–406

Everett ME (2013) Near-surface applied geophysics. Cambridge University Press, New York

Ferrucci F, Amelio M, Sorriso-Valvo M, Tansi C (2000) Seismic prospecting of a slope affected by deep-seated gravitational slope deformation: the Lago Sackung, Calabria, Italy. Eng Geol 57:53–64

Gill JC, Malamud BD (2014) Reviewing and visualizing the interactions of natural hazards. Rev Geophys 52:680–722

Jongmans D, Garambois S (2007) Geophysical investigation of landslides: a review. Bull Soc Geol France 178(2):101–112

Kearey P, Brooks M, Hill I (2001) An introduction to geophysical exploration. Blackwell Science, Malden

Kearey P, Brooks M, Hill I (2002) An introduction to geophysical exploration. Blackwell, Oxford, p 262

Lu N, Likos W, Wayllace A, Godt J (2010) Modified direct shear apparatus for unsaturated sands at low suction and stress. Geotech Test J 33(4):286–298

Lu N, Mitchell JK (2019) Geotechnical fundamentals for addressing new world challenges. Springer Series in Geomechanics and Geoengineering [Internet]. Available from: https://doi.org/10.1007/978-3-030-06249-1

McCann DM, Forster A (1990) Reconnaissance geophysical methods in landslide investigations. Eng Geol 29:59–78

Meric O, Garambois S, Jongmans D, Wathelet M, Chatelain JL, Vengeon JM (2005) Application of geophysical methods for the investigation of the large gravitational mass movement of Séchilienne. France Can Geotech J 42:1105–1115

NBRO (2016) Monitoring Report No.8 May 2016. NBRO. NBRO

NBRO (2019) Nature based landslide risk management project in Sri Lanka. National Building Research Organization, p. 18

Palacky G (1987) Resistivity characteristics of geological targets. In: Nabighian M (ed) Electromagnetic methods in applied geophysics-theory. Society of Exploration Geophysicists Tulsa, pp 53–129

Reynolds JM (1997) An introduction to applied and environmental geophysics. John Wiley and Sons, Chichester, p 806

Rolia E, Sutjiningsih D (2018) Application of geoelectric method for groundwater exploration from surface (A literature study). AIP Conference Proceedings, 1977

Saad R, Nawawi MNM, Mohamad ET (2012) Groundwater detection in alluvium using 2-D electrical resistivity tomography (ERT). Electr J Geotech Eng 17:369–376

Schmutz M, Albouy Y, Guérin R (2000) Joint electrical and time domain electromagnetism (TDEM) data inversion applied to the super sauze earthflow (France). Surv Geophys 21:371–390

Suzuki K, Higashi S (2001) Groundwater flow after heavy rain in landslide-slope area from 2-D inversion of resistivity monitoring data. Geophysics 66:733–743

Telford WM, Geldart LP, Sherif RE, Keys DA (1990) Applied geophysics. Cambridge University Press, Cambridge, p 770

Vander Velpen BPA, Sporry RJ (1993) Resist : a computer program to process resistivity sounding data on PC compatibles. Comput Geosci 19(5):691–703

Varnes DJ (1978) Slope movement types and processes. In: Schuster RL, Krizek RJ (eds) Landslides, analysis and control, special report 176: transportation research board. National Academy of Sciences, Washington, pp 11–33

Publisher's Note